Single Transverse Spin Asymmetries of Identified Charged Hadrons in Polarized p+p Collisions at $\sqrt{s} = 62.4$ GeV

I. Arsene[9], I. G. Bearden[4], D. Beavis[1], S. Bekele[8], C. Besliu[7], B. Budick[3], H. Bøggild[4], C. Chasman[1], H. H. Dalsgaard[4], R. Debbe[1], B. Fox[1], J. J. Gaardhøje[4], K. Hagel[5], A. Jipa[7], E. B. Johnson[8], R. Karabowicz[2], N. Katryńska[2], E. J. Kim[8], T. M. Larsen[4], J. H. Lee[1], G. Løvhøiden[9], Z. Majka[2], M. Murray[8], C. Nygaard[4], J. Natowitz[5], B. S. Nielsen[4], D. Pal[8], A. Qviler[9], C. Ristea[4], D. Röhrich[6], S. J. Sanders[8], P. Staszel[2], T. S. Tveter[9], F. Videbæk[1], H. Yang[6], and R. Wada[5]

The BRAHMS Collaboration

[1] Brookhaven National Laboratory, Upton, New York 11973

[2] Smoluchkowski Inst. of Physics, Jagiellonian University, Krakow, Poland

[3] New York University, New York 10003

[4] Niels Bohr Institute, Blegdamsvej 17, University of Copenhagen, Copenhagen 2100, Denmark

[5] Texas A&M University, College Station, Texas, 17843

[6] University of Bergen, Department of Physics, Bergen, Norway

[7] University of Bucharest, Romania

[8] University of Kansas, Lawerence, Kansas 66049

[9] University of Oslo, Department of Physics, Oslo, Norway

The first measurements of x_F-dependent single spin asymmetries of identified charged hadrons, $\pi^{\pm}$, $K^{\pm}$, and protons, from transversely polarized proton-proton collisions at 62.4 GeV at RHIC are presented. The measurements extend to high-x_F ($|x_F| \sim 0.6$) in both the forward and backward directions. Large asymmetries are seen in the pion and kaon channels. The asymmetries in inclusive π^+ production, $A_N(\pi^+)$, increase with x_F from 0 to $\sim$0.25 and $A_N(\pi^-)$ decrease from 0 to $\sim$−0.4. Even though K^- contains no valence quarks, observed asymmetries for K^- unexpectedly show positive values similar to those for K^+, increasing with x_F, whereas proton asymmetries are consistent with zero over the measured kinematic range. Comparisons of the data with predictions of QCD-based models are presented. The flavor dependent single spin asymmetry measurements of identified hadrons allow for stringent tests of theoretical models of partonic dynamics in the RHIC energy regime.

PACS numbers: 13.85.Ni, 13.88+e, 12.38.Qk

The transverse spin dependence of hadron cross-setions in $p^{\uparrow} + p$ ($\bar{p}^{\uparrow} + p$) reactions in the energy regime where perturbative QCD (pQCD) is applicable are expected to be negligibly small [1] in the lowest-order QCD approximation, whereas experimentally large left-right asymmetries have been observed [2–4] for large Feynman-x, $x_F = 2p_L/\sqrt{s}$. Measurements of large asymmetries of inclusive pion production and polarization in the production of hyperons [5] in a wide energy range have motivated various theoretical efforts to understand the phenomena. Observed large asymmetries are not particularly new phenomena in $p^{\uparrow} + p$ reactions since sizable asymmetries in inclusive pion production had been observed in the lower energy regime [6, 7], but understanding asymmetries in hadron reactions where a partonic QCD describes unpolarized cross-sections poses a new theoretical challenge. The main theoretical focus to account for the observed Single Spin Asymmetries (SSAs) in the framework of QCD has been on the role of transverse momentum dependent (TMD) partonic effects in the structure of the initial transversely polarized nucleon ("Sivers" mechanism) [8] and on the fragmentation process of a polarized quark into hadrons ("Collins" mechanism) [9]. Higher twist effects ("twist-3") arising from quark-gluon correlation effects beyond the conventional twist-2 distribution have also been considered as a possible origin of SSA [10, 11]. Recently, new measurements of SSAs have become available from semi-inclusive deep-inelastic scattering (SIDIS) [12, 13] and $p^{\uparrow}+p$ at RHIC providing more insight into the fundamental mechanisms of SSA as well as the relevant hadron structure. SSA measurements in $p^{\uparrow} + p$ at RHIC energies are of particular interest because the next-to-leading-order (NLO) pQCD calculations [14] for the unpolarized (spin-averaged) meson cross-sections at forward rapidities successfully describe the data [15, 16]. At $\sqrt{s} \sim$ 20 GeV where FNAL/E704 observed large SSAs, NLO pQCD cross-section calculations [14] significantly underpredict the measurements showing increasing discrepancies with increasing x_F [17]. The disagreements indicate that there is another mechanism, likely related to "soft" processes, which is significantly responsible for pion production at this lower energy. The two sets of data at $\sqrt{s}$ $\sim$ 20 GeV and at $\sqrt{s} = 200$ GeV cover a similar kinematic range in x_F and p_T and the measurements show that SSAs for pions are energy independent to first approximation. Since pQCD description of cross-sections at the high-energy region is quite successful, while it fails

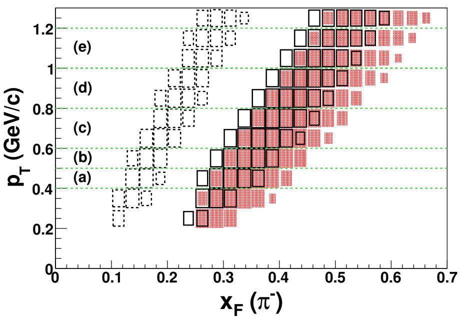

FIG. 1: p_T vs. x_F for the data used in the SSA analysis at $\sqrt{s} = 62.4$ GeV. The dotted boxes are for the measurements from FS at 6°, the filled boxes are from FS at 2.3° and the empty boxes with solid line are from 3°. Data from FS at 2.3° and 3° are used in combination for kaons and protons. The size of the boxes represents the relative intensity of the data in logarithmic scale. The 5 bands marked as (a)-(e) are the p_T ranges used in the Fig. 3.

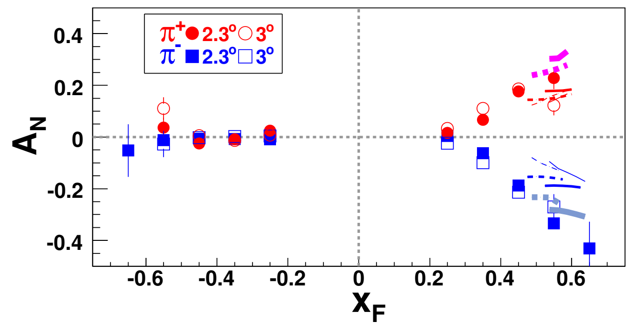

FIG. 2: A_N vs. x_F for π^+ and π^- at $\sqrt{s} = 62.4$ GeV for positive and negative x_F. Circle symbols are for π^+ and box symbols are for π^- measured in FS at 2.3° (solid symbols) and 3° (open symbols). The curves are from theoretical calculations. Solid lines are to be compared with the data at 2.3° and dotted lines are for 3°. Thick (solid and dotted) lines are from the initial-state Twist-3 calculations [23, 25], medium lines are from the final-state Twist-3 calculations [26, 27]. Predictions from the Sivers function calculations are shown as thin lines [28, 29]. Only statistical errors are shown where larger than symbols.

at the low energy domains, it might imply that the dominant mechanism responsible for the large SSAs at the two different energies are a manifestation of two different phenomena. The newly available measurements from RHIC in the intermediate energy regime at $\sqrt{s} = 62.4$ GeV in $p^\uparrow + p$ can uniquely provide an opportunity to clarify the pQCD contribution to SSAs and their energy dependences. A simultaneous description of SSAs and the unpolarized cross-sections [18] in a wide kinematic range will be a crucial test for the partonic pQCD description. In particular, flavor dependent SSA measurements allow more complete and stringent tests of theoretical models due to flavor dependence in parton distribution functions and fragmentation processes. We present here the first measurement of x_F-dependent SSAs of identified charged hadrons, $\pi^\pm$, $K^\pm$, and protons, from transversely polarized proton-proton collisions at 62.4 GeV at RHIC.

The SSA is defined as a "left-right" asymmetry of produced particles from the hadronic scattering of transversely polarized protons by unpolarized protons. Experimentally the asymmetry can be obtained by flipping the spins of polarized protons, and is customarily defined as analyzing power A_N:

$$A_N = \frac{1}{\mathcal{P}} \frac{(N^+ - \mathcal{L}N^-)}{(N^+ + \mathcal{L}N^-)}, \qquad (1)$$

where $\mathcal{P}$ is polarization of the beam, $\mathcal{L}$ is the spin dependent relative luminosity ($\mathcal{L} = \mathcal{L}_+/\mathcal{L}_-$) and $N^{+(-)}$ is the number of detected particles with beam spin vector oriented up (down). Since both colliding beams are polarized at RHIC, the polarization of "target" protons is averaged over in Eq. 1. The systematic error on the A_N measurements is estimated to be 10% including uncertainties from the beam polarization, $\delta\mathcal{P}/\mathcal{P} \sim 7.2\%$ for the "Blue" beam (circulating clockwise) and 9.3% for the "Yellow" beam (circulating counter-clockwise). The polarization of the Blue (Yellow) beam is utilized for the A_N measurements of particles in positive (negative) x_F. The systematic error represents mainly scaling uncertainties on the values of A_N. The average polarization of the beam $\mathcal{P}$ measured by the Hydrogen Jet and pC polarimeters is about 50% for the Blue and Yellow beams [19, 20].

The data presented here were collected by the BRAHMS detector system [21] with polarized $p+p$ collisions from RHIC Run VI with a sampled integrated luminosity of 0.21 pb^{-1} at $\sqrt{s} = 62.4$ GeV. The relative luminosity ($\mathcal{L}$) between the sums of spin-up and spin-down bunches was measured using the "CC" counter which uses a set of Cherenkov radiators placed symmetrically with respect to the nominal interaction point [16]. The detectors cover the pseudo-rapidity (η) interval from $3.26 < |\eta| < 5.25$, and are measured from Vernier scans to be sensitive to ~33% of the total inelastic cross-section of 36 mb at 62.4 GeV. The uncertainty of determining the relative luminosities is estimated to be 0.3%. The estimation was made by comparing relative luminosities measured by other global detectors, the Beam-Beam Counters and the Zero-Degree Calorimeters.

The Forward Spectrometer (FS) in BRAHMS has the unique capability of measuring charged particle tracks in the forward kinematic region ($\theta = 2.3° - 15°$) with good momentum resolution and particle identification. It consists of 4 dipole magnets, D1-D4 with a bending power of up to 9.2 Tm. The spectrometer has 5 tracking stations T1 through T5 positioned between the magnets. T1 and T2 are TPCs placed in front of and after the second dipole D2. T3,T4 and T5 are drift chambers with excellent position resolution ($\approx 80\mu m$) with T3 in front of D3, T4 between D3 and D4, and T5 after D4 and just in front of the the Ring Imaging Cherenkov Detector (RICH) [22].

The FS spectrometer settings used for SSA measure-

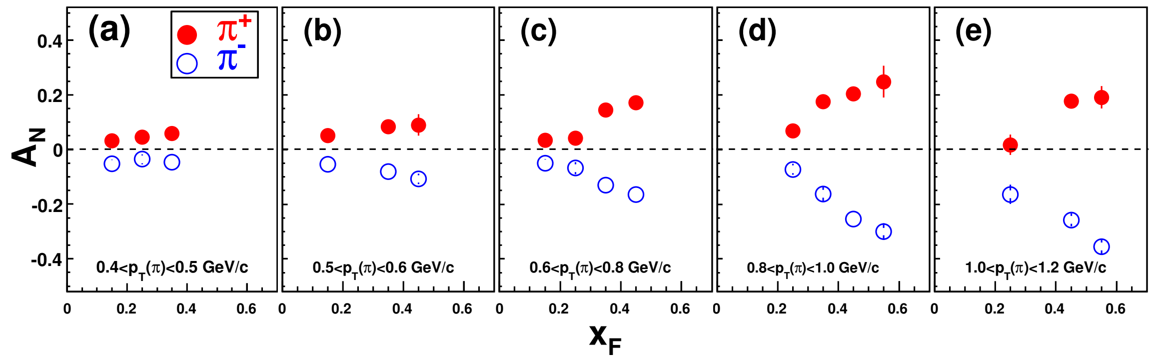

FIG. 3: A_N vs. x_F for π^+ and π^- at $\sqrt{s} = 62.4$ GeV for positive x_F at fixed p_T values: (a)$0.4 < p_T < 0.5$, (b)$0.5 < p_T < 0.6$, (c)$0.6 < p_T < 0.8$, (d)$0.8 < p_T < 1.0$, and (e)$1.0 < p_T < 1.2$ GeV/c as shown in Fig. 1, respectively.

ments were the FS at 2.3° and 3° at half of the maximum magnetic field and 6° at 25% of the maximum field for optimal acceptance. The momentum (p) resolution of the FS at the setting is $\delta p/p \approx 0.0016p$ ($\approx 0.0032p$) for the half field (quarter field) setting where p is in GeV/c. Particle identification was done by utilizing the RICH detector which is capable of identifying pions and kaons up to $p \sim 35$ GeV/c and protons above 17 GeV/c. The kinematic coverage of the data taken with the FS at 2.3°, 3° and 6° as a function of p_T and x_F are shown in Fig. 1, where the narrow p_T-x_F correlated band at a given setting is due to the small aperture of the spectrometer. A detailed description of the spectrometer and other experimental details can be found in [21].

The analyzing power A_N for charged pions, $A_N(\pi^+)$ and $A_N(\pi^-)$ at $\sqrt{s} = 62.4$ GeV as a function of x_F is shown in Fig. 2 for the two FS angle settings, 2.3° and 3°. At a fixed x_F value, the 3° setting samples higher p_T pions as indicated in Fig. 1. The mean p_T values $\langle p_T \rangle$ at x_F=0.55 are 1.08 and 1.28 GeV/c at 2.3° and at 3°, respectively. The measured A_N values show strong dependence in x_F reaching large asymmetries up to ∼40% at $x_F \sim 0.6$ and no significant asymmetries at $-x_F$. The decrease of A_N at high-p_T (>∼1 GeV/c) and high-x_F, especially for π^+, as shown in Fig. 2 by comparing the two sets of measurements at 2.3° and and at 3° might indicate that A_N is in accordance with the expected power-suppressed nature of A_N [23]. The asymmetries and their x_F-dependence are qualitatively in agreement with the measurements from E704/FNAL at $\sqrt{s} = 19.3$ GeV and also most recent $A_N(\pi^0)$ measurements at RHIC $\sqrt{s} = 200$ GeV [3, 15]. Figure 2 also compares $A_N(\pi)$ with a pQCD calculation in the range of $p_T > 1$ GeV/c using "extended" twist-3 parton distributions [10] including the "non-derivative" contributions [23–25]. In this framework, results of two calculations from the model are compared with the data: One is with only two quark valence densities (u_v,d_v) in the ansatz, which is shown in Fig. 2. Including additional sea- and anti- quark contributions in the model fit slightly increases $A_N(\pi)$ (∼5%). As the calculations show, the dominant contribution to SSA is from valence quarks with contributions from sea- and anti- quarks small enough that the current measurements are not able to quantitatively constrain the contribution. The calculations, which were done in the same kinematic range as the data, describe the data, especially $A_N(\pi^-)$ within the uncertainties. $A_N(\pi)$ calculated from the "final-state twist-3" which uses twist-3 fragmentation function for the pion under-predicts the data [26]. In Fig. 2, the data are also compared with calculations including Sivers mechanism which successfully describe the FNAL/E704 A_N data. The calculations use valence-like Sivers functions [28, 29] for u and d quarks with opposite sign. The fragmentation functions used are from the KKP parameterization [30], but the Kretzer fragmentation function [31] gives similar results. The calculations, as seen in the figure, underestimate A_N, which indicates that TMD parton distributions are not sufficient to describe the SSA data at this energy. All $A_N(\pi)$ calculations compared with the data shows $|A_N(\pi^+)| \sim |A_N(\pi^-)|$ while the data exhibit $|A_N(\pi^+)| < |A_N(\pi^-)|$ where $p_T \gtrsim 1$ GeV/c. Since there is a strong kinematic correlation between x_F and p_T in the data as shown in Fig. 1, the rise of A_N in Fig. 2 can be also driven by p_T.

Fig. 3 shows $A_N(\pi^+)$ and $A_N(\pi^-)$ for 5 different p_T regions from 0.4 to 1.2 GeV/c. As seen in Fig. 3, the x_F dependence of A_N at low-p_T ($p_T \lesssim 0.5$ GeV/c) is very small but increases with p_T in the kinematic region where the measurement has statistical significance ($p_T \lesssim 1$ GeV/c). The p_T-dependence of analyzing powers with x_F is qualitatively consistent with the measurements at $\sqrt{s} = 19.3$ GeV, where strong x_F dependent SSAs is observed only above a p_T "threshold" ($\lesssim$ 0.7 GeV/c) [3]. It is noted that the trend is also qualitatively in agreement with the polarization of the Λs produced at the same collision energy, $\sqrt{s} = 62.4$ GeV [5]. The SSAs for charged kaons as a function of x_F are shown in Fig. 4 together with twist-3 and Sivers calculations (see the figure caption for details). The asymmetry for $K^+(u\bar{s})$ is positive as is the A_N of $\pi^+(u\bar{d})$, which is expected if the asymmetry is mainly carried by valence quarks, but the measured positive SSAs of $K^-(\bar{u}s)$ seem to contradict the näive expectations [32] of valence quark dominance. In a valence-like model (no Sivers effect from sea-quarks

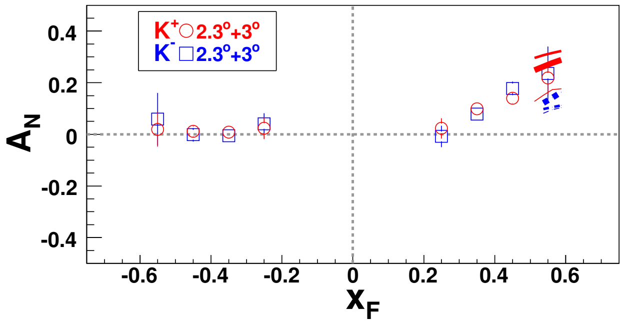

FIG. 4: $A_N(K^+)$ and $A_N(K^-)$ vs. x_F at $\sqrt{s} = 62.4$ GeV for positive and negative x_F. Circle symbols are for K^+ and box symbols are for K^-. The solid (K^+) and dotted (K^-) lines are from the initial-state twist-3 calculations with (thick lines) and without (medium lines) sea- and anti-quark contribution. Calculations for the Sivers function are shown as thin lines. Errors are statistical only.

and/or gluons), non-zero positive $A_N(K^-)$ implies large non-leading fragmentation functions (D_u^{K-}, D_d^{K-}) and insignificant contribution from strange quarks. Twist-3 calculations also under-predict $A_N(K^-)$ due to the small contribution of sea and strange-quark contribution to A_N in the model. The current calculations for kaon asymmetries at 62.4 GeV need an extra or a different mechanism to account for positively non-zero $A_N(K^-)$ at similar level of $A_N(K^+)$ as shown in Fig. 4.

SSAs at $x_F < 0$ probe the kinematics of the sea (gluon) region of $p^\uparrow$ at small-x and the valence region of p, which was experimentally measured by the produced particles in the forward hemisphere of p in the $p+p^\uparrow$ collisions utilizing the polarization information of the "target". The measured insignificant A_N for pions and kaons in large $|x_F|$ when $x_F < 0$, where $\hat{u} \to 0$ [33], indicates no significant contribution to A_N from processes where gq scattering is enhanced, and the asymmetries are dominated by the processes when $\hat{t}$ is small where large quark PDF and FF are expected.

In Fig. 5, we demonstrate that inclusive protons show no significant asymmetries in contrast to pions and kaons in the same kinematic region. The insignificant asymmetries observed are consistent with the measurements at lower energies [2, 34], but require more understanding of their production mechanism to theoretically describe the behavior because a significant fraction of the protons might still be related to the polarized beam fragments under the constraint of baryon conservation at this kinematic range [16].

In summary, BRAHMS has measured SSAs for inclusive identified charged hadron production at forward rapidities in $p^\uparrow+p$ at $\sqrt{s} = 62.4$ GeV. A twist-3 pQCD model describes the x_F dependence of $A_N(\pi)$ and the energy dependence at high p_T ($p_T > 1$ GeV/c) where the calculations are applicable, but it remains a challenge for pQCD models to consistently describe spin-averaged cross-sections at this energy [17, 18]. Measurements of A_N for kaons and protons suggest the possible manifestation of non-pQCD phenomena and call for more theoretical modeling with improved understanding of the fragmentation processes. The energy and flavor dependent asymmetry measurements impose an important constraint on theoretical models describing fundamental mechanisms of transverse spin asymmetries and the Quantum Chromodynamical description of hadronic structure.

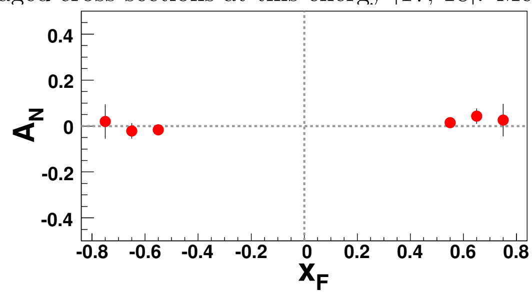

FIG. 5: A_N vs. x_F of the proton for positive and negative x_F.

We thank Feng Yuan, Umberto D'Alesio and Yuji Koike for providing us with their calculations shown in this letter. We also thank the RHIC Operation, Computing Facility, and Polarimeter Groups at BNL. This work was supported by Brookhaven Science Associates, LLC under Contract No. DE-AC02-98CH10886 with the U.S. Department of Energy, the Danish National Science Research Council, the Research Council of Norway, the Polish State Commission of Scientific Research and the Romanian Ministry of Research, and a sponsored research grant from Renaissance Technologies Corporation.

[1] G.L. Kane, J. Pumplin and W. Repko, *Phys. Rev. Lett.* **41** 1689 (1978).

[2] S. Saroff *et al.*, *Phys. Rev. Lett.* **64** 995 (1990).

[3] D.L. Adams *et al.* (E704 Collaboration), *Phys. Lett.* **B264** 462 (1991).

[4] A. Bravar *et al.* (E704 Collaboration), *Phys. Rev. Lett.* **77** 2626 (1996).

[5] S.M. Smith *et al.* (E608 Collaboration) *Phys. Lett.* **B185** 209 (1987).

[6] W.H. Dragoset, Jr. *et al.*, *Phys. Rev.* **D18** 3939 (1978).

[7] J. Antille *et al.*, *Phys. Lett.* **B94** 524 (1980).

[8] D. Sivers, *Phys. Rev.* **D41** 83 (1990).

[9] J.C. Collins, *Nucl. Phys.* **B396** 161 (1993).

[10] J. Qiu and G. Sterman, *Phys. Rev.* **D59** 014004 (1999).

[11] For a review, see J. Kodaira and K. Tanaka, *Prog. Theor. Phys.* **101** 191 (1999).

[12] A. Airapetian *et al.*, (HERMES Collaboration) *Phys. Rev. Lett.* **94** 012002 (2005).
[13] V.Yu. Alexakhin *et al.*, (COMPASS Collaboration) *Phys. Rev. Lett.* **94** 202002 (2005).
[14] B. Jager *et al.*, *Phys. Rev.* **D67** 054005 (2003).
[15] J. Adams *et al.* (STAR Collaboration), *Phys. Rev. Lett.* **92** 171801 (2004).
[16] I. Arsene *et al.* (BRAHMS Collaboration) *Phys. Rev. Lett.* **98** 252001 (2007).
[17] C. Bourrely and J. Soffer, *Eur. Phys. J.* **C36** 371 (2004).
[18] BRAHMS Collaboration, Cross-section measurements of identified hadrons at forward rapidities at $\sqrt{s} = 62.4$ GeV, in preparation; F. Videbæk, Proc. of 23rd Winter Workshop on Nuclear Dynamics, Feb. 2007, Big Sky, USA.
[19] RHIC CNI Polarimeter Group: http://www.rhic.bnl.gov/~cnipol/
[20] H. Okada *et al.*, Proc. of the XIIth International Workshop on Polarized Sources, Targets & Polarimetry; PSTP07, Sep. 2007, Upton, USA, arXiv:0712.1389 (2007).
[21] M. Adamczyk *et al.* (BRAHMS Collaboration), *Nucl. Instr. Meth.* **A499** 437 (2003).
[22] R. Debbe *et al.*, *Nucl. Instr. Meth.* **A570** 216 (2007).
[23] C. Kouvaris *et al.*, *Phys. Rev.* **D74** 1104013 (2006).
[24] W. Vogelsang, Proc. of 17th International Spin Physics Symposium, SPIN2006, Oct. 2006, Kotyo, Japan.
[25] The calculations were provided by Feng Yuan.
[26] Y. Koike, Proc. of 15th International Spin Physics Symposium, SPIN2002, Sep. 2002, Upton, USA.
[27] The calculations were provided by Yuji Koike.
[28] U. D'Alesio and F. Murgia, *Phys. Rev.* **D70** 074009 (2004), Proc. of 17th International Spin Physics Symposium, SPIN2006, Oct. 2006, Kotyo, Japan
[29] The calculations were provided by Umberto D'Alesio.
[30] B.A. Kniehl *et al.*, *Nucl. Phys.* **B597** 337 (2001).
[31] S. Kretzer, *Phys. Rev.* **D62** 054001 (2000).
[32] M. Anselmino *et al.*, *Phys. Lett.* **B442** 470 (1998).
[33] $\hat{u}$ and $\hat{t}$ are invariant variables defined as $(p_b - p_c)^2$ and $(p_a - p_c)^2$ respectively for the parton subprocesses in $p^\uparrow + p \to \pi(K) + X$ or $p + p^\uparrow \to \pi(K) + X$ in terms of $a + b \to c + d$ where c fragments into $\pi(K)$.
[34] V. Abramov *et al.*, Proc. of 16th International Spin Physics Symposium, SPIN2004, Oct. 2004, Trieste, Italy.